Flutter and Buckling of General Laminated Plates

James Wayne Sawyer*
NASA Langley Research Center, Hampton, Va.

An anisotropic analysis and solution procedure has been developed using linear small-deflection theory for the buckling and flutter of finite, simply supported laminated plates with arbitrary fiber orientations. The extended Galerkin method is used to obtain approximate solutions to the coupled governing equations. Calculations show that both bending-extensional coupling and bending-twisting stiffness terms have a destabilizing effect on buckling and flutter. This effect is most pronounced when the number of layers is small. However, for plates with a sufficient number of layers, the coupling and bending-twisting stiffness terms have negligible effect and orthotropic plate theory is applicable. For symmetric plates, the number of layers required for orthotropic plate theory to be applicable is generally less for the buckling problem than for flutter. The direction of airflow over the plate surface has a significant effect on flutter and hence on the fiber orientation that gives the highest flutter dynamic pressure.

Nomenclature

A_{ij} = extensional stiffnesses
A^* = A^{-1}
a,b = plate dimensions along x and y axis, respectively
B_{ij} = coupling stiffnesses
B^* = $-A^{-1}B$
D_{ij} = bending stiffnesses
D^*_{ij} = $D-BA^{-1}B$
$\bar{D}_{11}$ = D_{11} with all $\theta=0$ deg
E_{11},E_{22} = principal Young's moduli in one and two directions, respectively
F = Airy stress function
G_{12} = shear modulus in 1-2 plane
M_∞ = Mach number
N = number of layers in plate
$\bar{N}_x,\bar{N}_y$ = applied inplane normal loads per unit length in x and y directions, respectively
$\bar{N}_{xy}$ = applied inplane shearing loads per unit length
q = dynamic pressure of airstream
w = normal displacements
x,y,z = Cartesian coordinates
β = compressibility factor, $\sqrt{M_\infty^2-1}$
γ = plate mass per unit area
θ = rotation angle of the fibers with respect to the plate axis
θ_{opt} = value of θ that results in highest flutter dynamic pressure
Λ = crossflow angle
λ = $2qa^3/\beta\bar{D}_{11}$, flutter parameter
$\bar{\lambda}$ = flutter parameter given by orthotropic plate theory
ν_{12},ν_{21} = Poisson's ratio for orthotropic lamina such that $\nu_{12}E_{22}=\nu_{21}E_{11}$

COMPOSITE materials are being considered for a wide variety of applications, but to use them efficiently a good understanding of their structural and dynamic behavior under various load conditions is needed. Plates formed by bonding several layers of composite material together are of particular interest. For general laminated composite plates, where the number of layers and the fiber orientation are arbitrary, coupling between bending and extension and bending and twisting both in the governing differential equations and the boundary conditions can produce significant effects that are not accounted for in classical plate theory. The difficulty of obtaining solutions to the coupled equations has limited current understanding of the structural and dynamic behavior of general laminated composite plates.

Several buckling analyses have been made for finite plates that considered the effects of either bending-extension coupling[1] or bending-twisting coupling,[2] but simultaneous effects have not been shown except for infinitely long plates[3] even though some finite-difference and finite-element analyses[4,5] are available that have the capability. Furthermore, although panel flutter has been recognized for some time as a potential problem in the design of plates subjected to supersonic flow, the flutter characteristics of laminated composite plates are not well defined,[6-8] and the designer has had to rely on classical orthotropic plate theory.[9] In this paper, an anisotropic buckling and flutter analysis has been developed taking into account both the bending-extension coupling and the bending-twisting coupling. Parametric studies have been conducted using the anisotropic analysis to determine the effects of various anisotropic stiffness parameters on the static and dynamic stability of laminated plates and to assess the range of applicability of classical orthotropic plate theory.

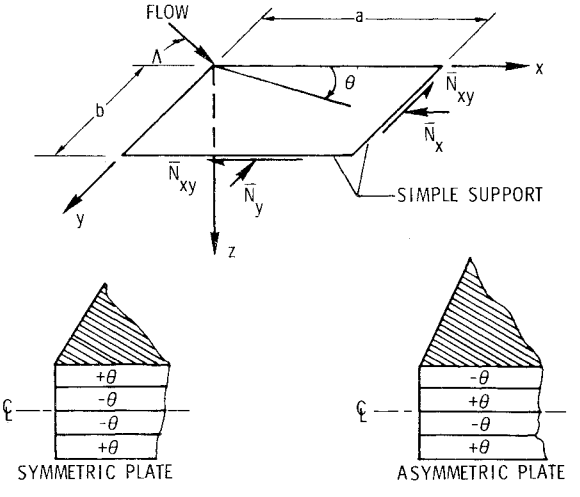

Fig. 1 Plate geometry and coordinate system.

Presented at the AIAA/ASME/SAE 17th Structures, Structural Dynamics and Materials Conference, King of Prussia, Pa., May 5-7, 1976 (in bound volume of Conference papers, no paper number); submitted May 12, 1976; revision received Dec. 1, 1976.

Index categories: Structural Stability Analysis; Structural Composite Materials (including Coatings).

*Aerospace Engineer, Space Transport Structures Section, Structures and Dynamics Division. Member AIAA.

Analysis

The analysis and solution procedure was developed using the linear small-deflection theory for simply supported general laminated plates. The plate geometry and coordinate system are shown in Fig. 1, as is the definition of fiber orientation for symmetrically layered and asymmetrically layered plates. For general laminated plates, the A, B, and D stiffness matrices are fully populated and relate the inplane forces and bending moments to the strains and curvatures. The relationship between the stiffness matrices and the laminae material properties are well known.[3] Assuming any Airy stress function that satisfies the inplane equilibrium equation, the governing equations derived from the lateral equilibrium and compatibility equations are given as follows.[10,11]

$$\left[B^*_{21}\frac{\partial^4 F}{\partial x^4}+(2B^*_{26}-B^*_{61})\frac{\partial^4 F}{\partial x^3\partial y}+(B^*_{11}+B^*_{22}-2B^*_{66})\frac{\partial^4 F}{\partial x^2\partial y^2}+(2B^*_{16}-B^*_{62})\frac{\partial^4 F}{\partial x\partial y^3}+B^*_{12}\frac{\partial^4 F}{\partial y^4}\right]+D^*_{11}\frac{\partial^4 w}{\partial x^4}+4D^*_{16}\frac{\partial^4 w}{\partial x^3\partial y}+2(D^*_{12}+2D^*_{66})\frac{\partial^4 w}{\partial x^2\partial y^2}+4D^*_{26}\frac{\partial^4 w}{\partial x\partial y^3}+D^*_{22}\frac{\partial^4 w}{\partial y^4}+\gamma\frac{\partial^2 w}{\partial t^2}$$
$$=\frac{-2q}{\beta}\left(\frac{\partial w}{\partial x}\cos\Lambda+\frac{\partial w}{\partial y}\sin\Lambda\right)-\bar{N}_x\frac{\partial^2 w}{\partial x^2}-\bar{N}_y\frac{\partial^2 w}{\partial y^2}-2\bar{N}_{xy}\frac{\partial^2 w}{\partial x\partial y} \tag{1}$$

$$A^*_{22}\frac{\partial^4 F}{\partial x^4}-2A^*_{26}\frac{\partial^4 F}{\partial x^3\partial y}+(2A^*_{12}+A^*_{66})\frac{\partial^4 F}{\partial x^2\partial y^2}-2A^*_{16}\frac{\partial^4 F}{\partial x\partial y^3}+A^*_{11}\frac{\partial^4 F}{\partial y^4}-\left[B^*_{21}\frac{\partial^4 w}{\partial x^4}+(2B^*_{26}-B^*_{61})\frac{\partial^4 w}{\partial x^3\partial y}+(B^*_{11}+B^*_{22}-2B^*_{66})\frac{\partial^4 w}{\partial x^2\partial y^2}+(2B^*_{16}-B^*_{62})\frac{\partial^4 w}{\partial x\partial y^3}+B^*_{12}\frac{\partial^4 w}{\partial y^4}\right]=0 \tag{2}$$

where the aerodynamic pressure terms in Eq. (1) are those given by linear piston theory[12] with flow at an arbitrary crossflow angle.

For simply supported edges, the bending moments and deflections at the plate edges are zero as expressed by the following equations.

$$w(0,y)=w(a,y)=w(x,0)=w(x,b)=0$$

$$\left[B^*_{11}\frac{\partial^2 F}{\partial y^2}+B^*_{21}\frac{\partial^2 F}{\partial x^2}-B^*_{61}\frac{\partial^2 F}{\partial x\partial y}\right]+D^*_{11}\frac{\partial^2 w}{\partial x^2}+D^*_{12}\frac{\partial^2 w}{\partial y^2}+2D^*_{16}\frac{\partial^2 w}{\partial x\partial y}\bigg|_{x=0,a}=0$$

$$\left[B^*_{12}\frac{\partial^2 F}{\partial y^2}+B^*_{22}\frac{\partial^2 F}{\partial x^2}-B^*_{62}\frac{\partial^2 F}{\partial x\partial y}\right]+D^*_{12}\frac{\partial^2 w}{\partial x^2}+D^*_{22}\frac{\partial^2 w}{\partial y^2}+2D^*_{26}\frac{\partial^2 w}{\partial x\partial y}\bigg|_{y=0,b}=0 \tag{3}$$

Additional boundary conditions are needed for the coupled equations and are obtained by requiring the induced inplane normal and shear loads to be zero at the plate edges as follows:

$$\frac{\partial^2 F}{\partial y^2}\bigg|_{x=0,a}=0 \tag{4a}$$

$$\frac{\partial^2 F}{\partial x^2}\bigg|_{y=0,b}=0 \tag{4b}$$

$$\frac{\partial^2 F}{\partial x\partial y}\bigg|_{\substack{x=0,a\\y=0,b}}=0 \tag{4c}$$

For general laminated plates, the equations and boundary conditions are coupled by the B_{ij} terms contained in the brackets. However, for plates constructed so that they are symmetric about their geometric midplane (see Fig. 1), the B_{ij} terms are all zero and the equations are uncoupled. Thus, for symmetric plates, only Eq. (1) and boundary conditions (3) need to be solved. Note that Eqs. (1) and (3) with $B_{ij}=0$ are the standard orthotropic plate-theory equations with the exception of the bending-twisting stiffness terms D^*_{16} and D^*_{26}. The magnitudes of these terms are dependent on the fiber orientation, the number of layers composing the plate, and the location of the reference surface; their values are zero for plates with fiber orientation angles of 0 and 90 deg. For other orientations with the reference surface at the midplane, the values approach zero as the number of repeated sequence of layers become large.

A double Fourier series representation of the transverse displacement and the stress function is used to obtain solutions to the coupled equations and boundary conditions. Since series functions that satisfy all the coupled boundary conditions are not known, the extended Galerkin method[13] is used as it allows solutions with well-known beam functions that satisfy only the natural boundary conditions. For simply supported boundary conditions, simple one-term trigonometric functions are adequate. A more detailed discussion of the solution procedure is given in Ref. 11. The procedure can be used to calculate natural vibration frequencies and inplane buckling loads, as well as the onset of flutter in the presence of applied uniform inplane normal and shear payloads. Although preloads can be accommodated, the displacements due to the preloads are neglected in the analysis.

Results and Discussion

Buckling and flutter calculations have been made for plates with elastic material properties typical of boron-epoxy, glass-epoxy, and graphite-epoxy materials. The specific material properties used in making the calculations are tabulated in Table 1 where the 1 and 2 subscripts refer to the principal axes of the material. Selected results from the calculations will be presented in the following discussion. Note that results are presented only for plates with identical material in each lamina. A sufficient number of modes have been used in the analysis to insure that the buckling and flutter results presented are converged to within 1%. Most of the results presented will be for each layer having the same absolute fiber orientation angle but with alternating signs. Since many panels being built are composed of layers with fiber orientation angles of 0, +45, and 90 deg, some results will also be presented for an unsymmetric plate with the following fiber orientations: 0, +45, 90, −90, −45, and 0 deg.

Table 1 Material Properties

Material	Boron-epoxy	Graphite-epoxy	Glass-epoxy
E_{11}/E_{22}	10	8.8	3
G_{12}/E_{22}	0.33	0.27	0.40
ν_{12}	0.3	0.3	0.3

Buckling

Inplane Buckling Loads

Static buckling solutions have been obtained from the bending and extensional equations [see Eqs. (1) and (2)] by setting the inertia and aerodynamic pressure terms equal to zero. Nondimensional inplane, longitudinal compressive buckling loads are shown as a function of fiber orientation in Fig. 2a and b for symmetric laminated plates with length/width ratios of 1 and 10, respectively. (Recall that for symmetric plates, the bending and extensional equations are uncoupled.) In the ordinate parameter, $\bar{D}_{11}$ is the plate-bending stiffness with all the fibers aligned at $\theta = 0$ deg. Thus, for a given thickness plate, the curves show the relative load-carrying ability as a function of the fiber orientation angle and the number of layers. Anisotropic results obtained using graphite-epoxy material properties are compared with results obtained using orthotropic plate theory shown by the dashed curves. Note that a buckling value is also given for the unsymmetric plate shown in the inset. For both a/b of 1 and 10, the highest buckling loads are obtained with the fibers rotated at approximately 45 deg to the plate axes. Note that the buckling value for the unsymmetric plate is lower than the maximum values obtained with all the fibers at ± 45 deg, but are higher than or approximately the same as the values obtained with all the fibers aligned with the plate axes. For plates with a small number of layers, the bending-twisting stiffness terms D_{16}^* and D_{26}^* are destabilizing and result in static buckling loads that are considerably lower than those predicted by orthotropic plate theory, which neglects these terms. Increasing the number of layers decreases the importance of the D_{16}^* and D_{26}^* terms and thus increases the static buckling loads. For $N \geq 6$ the terms become so insignificant that they can be neglected and orthotropic plate theory used with little error in the results. Note also that with the fibers aligned with the plate axes (i.e., $\theta = 0$ or 90 deg) the D_{16}^* and D_{26}^* terms are zero and orthotropic plate theory is in agreement with the present anisotropic theory for any number of layers.

Inplane Shear Buckling Loads

Nondimensional inplane shear buckling loads are shown as a function of the fiber orientation angle in Fig. 3a and b for symmetric graphite-epoxy, laminated plates with length/width ratios of 1 and 10, respectively. Results obtained for different numbers of layers N are compared with results obtained using orthotropic plate theory shown by the dashed curves. Two curves are shown for plates with the same number of layers depending on the direction of the fibers in the outer layer. The upper and lower set of solid curves, respectively, are for a favorable (i.e., in the direction of principal compression loads) and unfavorable (i.e., away from the direction of principal compression loads) orientation of the fibers in the outer layers. Maximum buckling loads are obtained for a favorable orientation of the fibers in the outer layers and for a rotation angle of 45 deg for the square plate (see Fig. 3a) and for approximately 60 deg for the $a/b = 10$ plate (see Fig. 3b). Decreasing the number of layers increases the buckling loads for plates with a favorable orientation of the fibers in the outer layers whereas the opposite is true for an unfavorable fiber orientation. However, in either case, increasing the number of layers results in the buckling values approaching those given by orthotropic plate theory. Note that for inplane normal loads, six layers were sufficient for orthotropic plate theory to give adequate buckling loads. However, for plates with six layers subjected to inplane shear loads, orthotropic plate theory gives buckling loads that are over 18% in error and may be either conservative or non-conservative depending on the orientation of the fibers in the outer layers or the direction of the shear load.

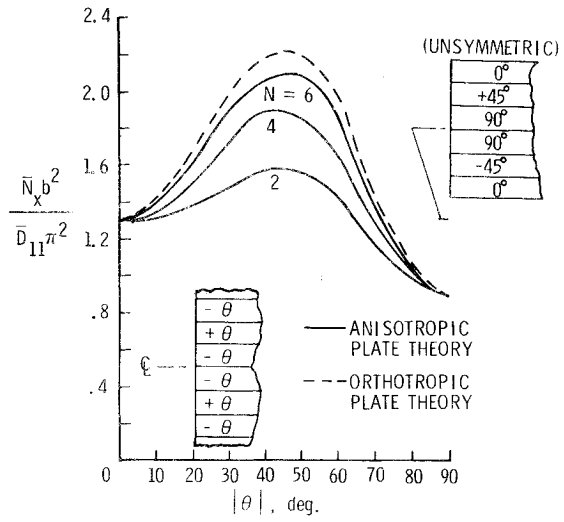

a) $a/b = 1.0$

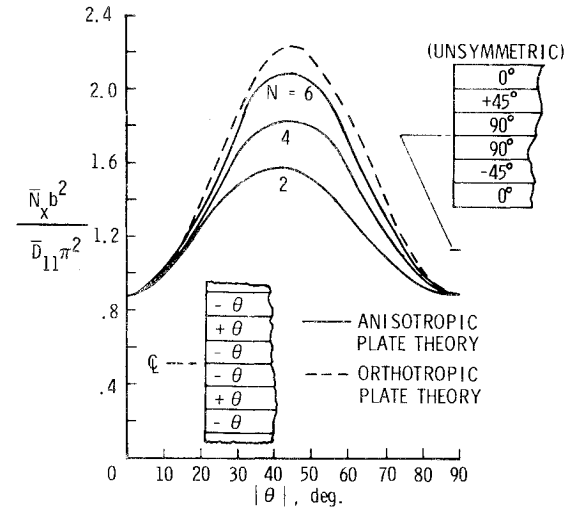

b) $a/b = 10.0$

Fig. 2 Buckling of symmetric graphite-epoxy plates with inplane normal loads, $\bar{N}_y = \bar{N}_{xy} = 0$.

Panel Flutter

Symmetric Plates

Flutter solutions are obtained from the bending and extensional equations when the inertia and aerodynamic terms are retained in Eq. (1). Flutter boundaries are shown as a function of fiber orientation in Figs. 4a-c for symmetric laminated plates with properties typical of glass-epoxy, graphite-epoxy, and boron-epoxy materials, respectively. In the ordinate parameter, q is the dynamic pressure of the stream. Results obtained for square plates with different numbers of layers N are compared with results obtained using orthotropic plate theory shown by the dashed curves. For each plate, the highest flutter dynamic pressure is obtained with the fibers aligned with the x axis (i.e, $\theta = 0$ deg). The reduction in the flutter dynamic pressure parameter for $\theta > 0$ deg is dependent on N and the material properties. For graphite-epoxy (see Fig. 4b) or boron-epoxy (see Fig. 4c) plates with a small number of layers, the bending-twisting stiffness terms have a pronounced destabilizing effect on the flutter stability but increasing the number of layers increases the flutter stability. For the glass-epoxy plate (see Fig. 4a), the bending-twisting stiffness terms have a much smaller destabilizing effect even for plates with a small number of layers. The smaller destabilizing effects of anisotropy and increasing θ for the glass-epoxy material are attributed to the more nearly equal values of modulus of elasticity in both directions for the

glass-epoxy material ($E_{11}/E_{22}=3.0$) as compared with the graphite-epoxy ($E_{11}/E_{22}=8.8$) and boron-epoxy ($E_{11}/E_{22}=10.0$) materials. For the remainder of the paper, only results obtained using boron-epoxy material properties will be discussed.

Flutter boundaries are shown as a function of fiber orientation in Fig. 5 for symmetric, boron-epoxy, laminated plates with a length/width ratio of 2.0. The bending-twisting stiffness terms have a destabilizing effect on the flutter boundaries similar to that noted for the square plate (see Fig. 4c). For the plate with a length/width ratio of 2.0, the highest value of the flutter dynamic pressure parameter is obtained with the fibers rotated at an angle to the x axis that varies between 30 deg and 45 deg and is dependent on the number of layers composing the plate. The flutter value shown for the unsymmetric plate with $N=6$ is lower than the maximum values obtained with all the fibers rotated by the same $|\theta|$ value and is approximately equal to the value obtained with $\theta=0$ deg. For both the square and the $a/b=2.0$ plates, ten or more layers are required for orthotopic plate theory to give flutter boundaries that are in reasonable agreement with the present anisotropic theory. Recall that for plates subjected to inplane normal buckling loads, only six layers are required for orthotropic plate theory to give good results.

Asymmetric Plates

For asymmetric plates, the bending and extensional governing equations are coupled and must be solved simultaneously. Flutter boundaries are shown in Fig. 6 for a square asymmetric plate. For this layer orientation, the bending-twisting-stiffness terms are zero and the differences in the flutter boundaries are due to bending-extensional coupling. For plates with a small number of layers, coupling has a large destabilizing effect on the flutter parameter, but for $N\geq 6$ the effect is small. Orthotropic plate theory does not consider bending-extensional coupling and thus shows good agreement with the present theory only for plates with a large number of layers. As was noted for the bending-twisting coupling, aligning the fibers with the plate axes (i.e., $\theta=0$ deg) removes the bending-extensional coupling and the present theory and orthotropic plate theory are in agreement.

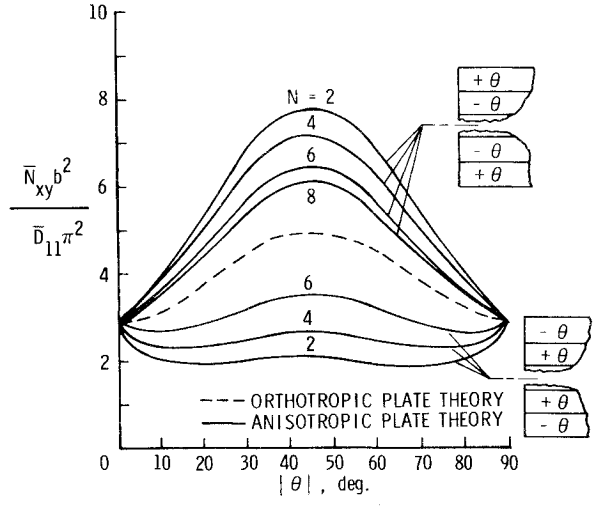

a) $a/b=1.0$

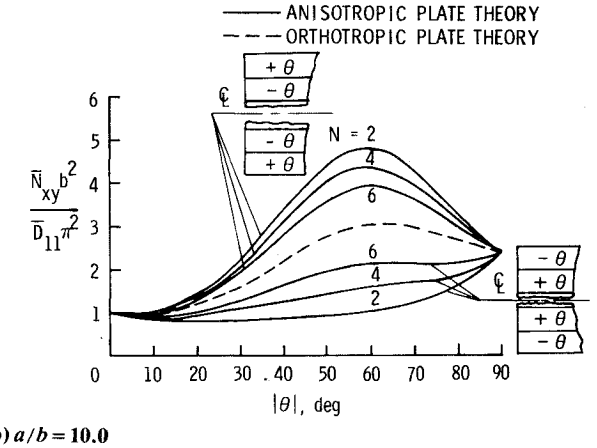

b) $a/b=10.0$

Fig. 3 Buckling of symmetric graphite-epoxy plates with inplane shear loads. $\bar{N}_x=\bar{N}_y=0$.

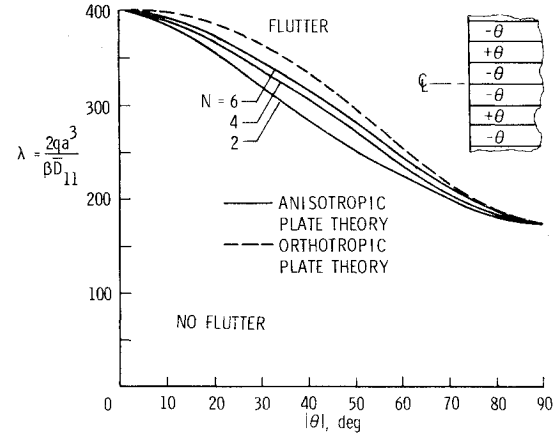

a) Glass-epoxy plate

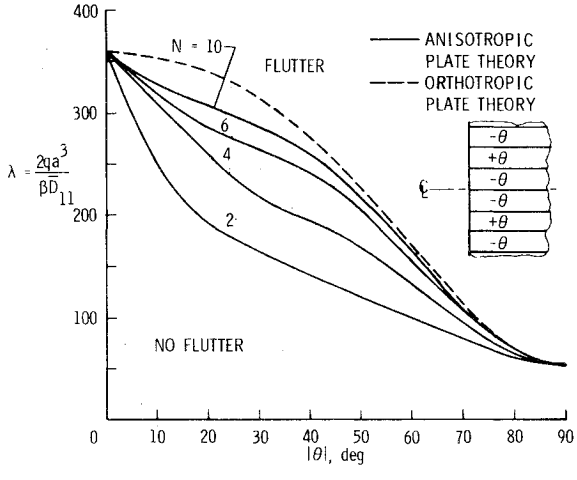

b) Graphite-epoxy plate

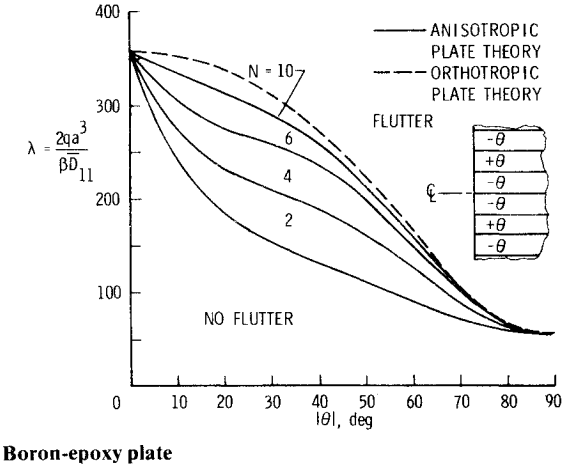

c) Boron-epoxy plate

Fig. 4 Flutter boundaries for square symmetric plates.

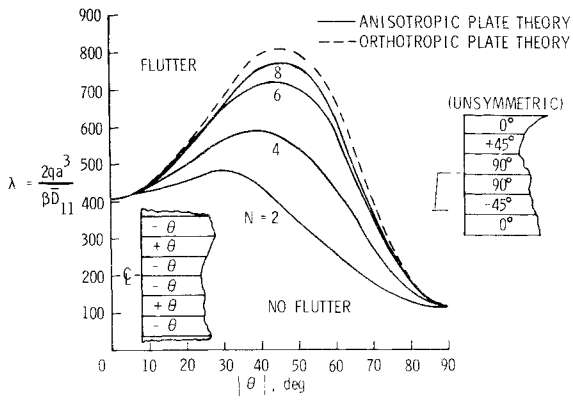

Fig. 5 Flutter boundaries for boron-epoxy symmetric plates with $a/b = 2.0$.

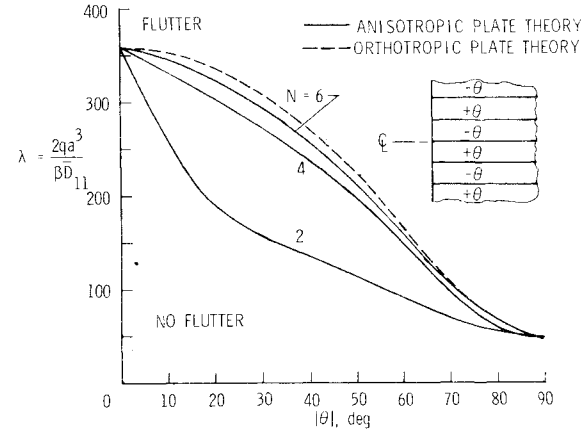

Fig. 6 Flutter boundaries for square, asymmetric, boron-epoxy plates.

Due to the simplicity and availability of orthotropic plate-theory solutions, it is most beneficial to know when orthotropic plate theory is adequate for flutter of laminated plates. The limitation of orthotropic plate theory for flutter is summarized in Fig. 7 for the square symmetric (solid curves) and asymmetric plates (dashed curves) discussed previously. The ratio of the dynamic pressure parameter obtained using the present analysis to that obtained using orthotropic plate theory is shown as a function of the number of layers of material for values of θ of 10, 15, 30, and 45 deg. Note that for the symmetric plates at least twelve layers are required for orthotropic plate theory to give flutter values that are within 10% of those given by the present anisotropic theory; however, for the asymmetric plates, only six layers are required for orthotropic plate theory values to be within 5% of those given by the present anisotropic analysis. Thus, bending-twisting coupling has a more adverse effect on the flutter of laminated plates than bending-extensional coupling. Consequently, orthotropic plate theory may be used for asymmetric plates with six or more layers. However, it is important to note that in all cases orthotropic plate theory is in error and unconservative, and should be used with caution. Also, for plates with variable material properties or layer thicknesses, the regions of applicability of orthotropic plate theory might be different.

General Laminated Plates

Flutter boundaries shown in the previous figures have been for fiber layers arranged either symmetrically or asymmetrically about the plate midplane. However, for general laminated plates, numerous possible arrangements exist. For example, with flow aligned with the plate axis, a composite plate with four identical layers of material with the principal direction of each layer making an angle of $\pm\theta$ with the plate axes can be arranged so as to make six configurations which have different flutter characteristics. Flutter boundaries are presented in Fig. 8 for four-ply square plates with the layers of material arranged in each of the six possible configurations. The highest flutter dynamic pressure parameter is obtained for the asymmetric plate with the layers arranged as $+\theta$ $-\theta+\theta-\theta$ or $-\theta+\theta-\theta+\theta$. For this arrangement of layers, only bending-extensional coupling is obtained. For other arrangements of the layers where bending-twisting coupling or bending-twisting and bending-extensional coupling are obtained, the flutter boundaries may be as much as 80% lower. The lowest flutter boundary is obtained for a symmetric plate with all the fibers aligned in the same direction.

Flow Angularity

For most practical applications, the direction of airflow over the plate surface will vary; consequently, the arrangement of the layers and the fiber orientation that gives the highest flutter dynamic pressure may be strongly dependent on the direction of flow. Flutter dynamic pressure is shown as a function of the fiber orientation angle in Fig. 9a and 9b for square plates with cross-flow angles of 15 and 30 deg, respectively. Curves are presented for the asymmetric and symmetric plates that for zero cross-flow were shown in Fig. 8 to have, respectively, maximum and minimum flutter boundaries. For the symmetric plate, separate curves are obtained for positive and negative fiber orientation angles. For cross-flow angles of 15 and 30 deg, the peak value of the flutter dynamic pressure for the symmetric plate is obtained for the fibers aligned with the flow (i.e., $\theta = 15$ deg for $\Lambda = 15$ deg and $\theta = 30$ deg for $\Lambda = 30$ deg). For the asymmetric plate, the highest flutter values occur at fiber orientation angles greater than the flow angle. In contrast to results obtained with zero cross flow, the symmetric plate with cross-flow angles of 15 and 30 deg has peak values of the flutter dynamic pressure that are higher than those obtained for the asymmetric plate. Note, however, that with cross-flow, the maximum flutter values are less than those obtained with the flow aligned with the plate axes. For negative or large positive fiber orientation angles, the symmetric plate has lower values of the flutter dynamic pressure than the asymmetric plate.

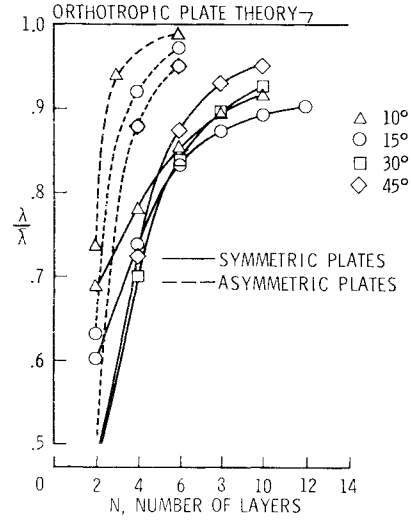

Fig. 7 Applicability of orthotropic plate theory for flutter of square boron-epoxy plates.

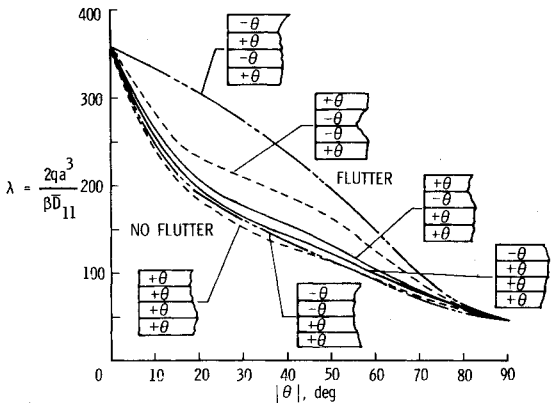

Fig. 8 Flutter boundaries for four-layer, square, boron-epoxy plates.

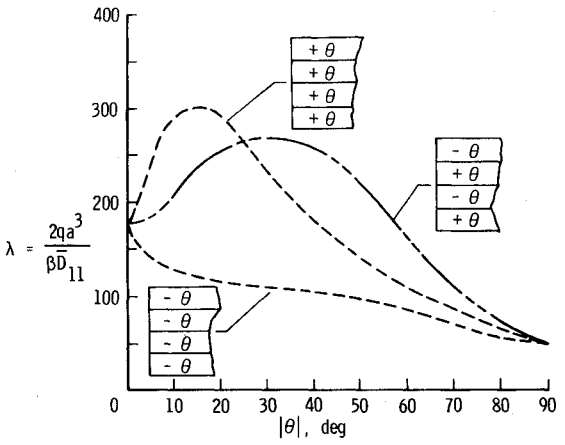

a) $\Lambda = 15$ deg

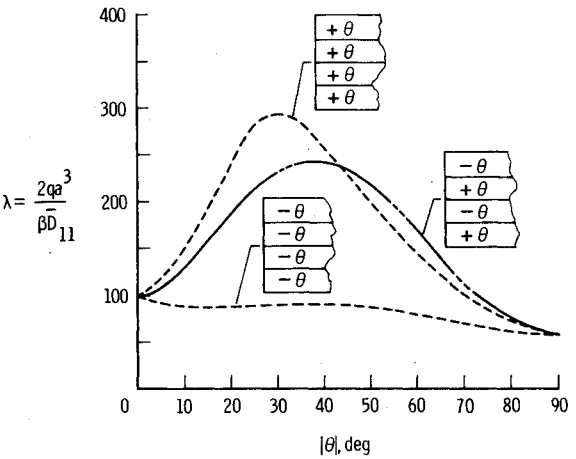

b) $\Lambda = 30$ deg

Fig. 9 Flutter of four-layer, square, boron-epoxy plate with crossflow.

Thus, Figs. 8 and 9 clearly show that in the design of laminated plates that will experience cross-flow, the fiber orientation angles and the arrangement of the layers may significantly influence the flutter resistance of the plate.

Mass Efficiency

It is of interest to assess the mass efficiency of composite plates compared with conventional plates from the standpoint of flutter resistance. This has been done in Fig. 10 where the plate unit mass per unit width is plotted for boron/epoxy

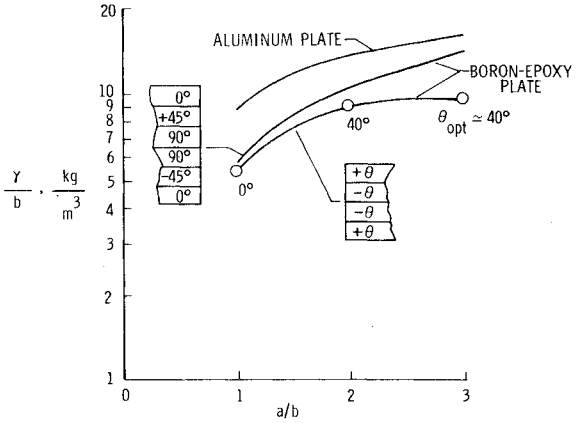

Fig. 10 Flutter critical mass of boron-epoxy and aluminum plates for $q/\beta = 55$ kN/m^2 and $\Lambda = 0$ deg.

laminated plates and aluminum isotropic plates as a function of a/b. The curves represent the least mass plates that resist flutter at a fixed value of $q/\beta = 55$ KN/m^2 and $\Lambda = 0$ deg. Curves for the boron-epoxy materials are shown for both symmetric and unsymmetric plates. The fiber orientation angles, θ_{opt}, for the symmetric plates were determined for each a/b to give the maximum resistance to flutter and are given on the curve. The unit mass for the symmetric plates given by the lower curve is approximately two-thirds that of an equivalent isotropic aluminum plate. This is approximately the same savings found for composite plates loaded in compression.[14] The unsymmetric plate with $N = 6$ shows substantial mass savings over an equivalent aluminum plate but requires considerable more mass than the symmetric plate for $a/b \geq 2.0$.

Concluding Remarks

For general laminated composite plates, the bending and extensional governing equations are coupled and have bending-twisting stiffness terms that are not considered in orthotropic plate theory. The extended Galerkin method is used to obtain approximate solutions to the coupled equations including the bending-twisting stiffness terms for simply supported general laminated plates. The aerodynamic pressure loading used in the analysis is that given by linear piston theory with flow at arbitrary cross-flow angle. The analysis has been used to study the effects of a limited number of parameters on the inplane normal and shear buckling loads and on the flutter boundaries for typical laminated plates. Calculations have been made primarily for plates with each layer having the same material properties and absolute value of the fiber orientation angle.

The limited calculations presented herein indicate that, for symmetric and asymmetric laminated plates with a large number of layers, the bending-extensional coupling and the bending-twisting stiffness terms can be neglected and orthotropic plate theory used. For plates with a small number of layers, orthotropic plate theory is usually nonconservative except for the shear buckling of plates with certain fiber orientations. Orthotropic plate theory gives good flutter results for plates with six or more layers arranged asymmetrically about the plate midplane, whereas twelve or more layers are required for it to be applicable to symmetric plates. For the normal buckling of symmetric plates, the number of layers required for orthotropic plate theory to be applicable is generally less than noted for the flutter problem. The direction of airflow over the plate surface has a significant effect on flutter and hence on the fiber orientation that gives the highest flutter dynamic pressure. For square plates, aligning the fibers with the flow generally results in the highet flutter dynamic pressure.

References

[1]Whitney, J. M. and Leissa, A. W., "Analysis of Heterogeneous Anisotropic Plates," *Journal of Applied Mechanics*, Vol. 36, 1969, pp. 261-266.

[2]Ashton, J. E. and Waddoups, M. E., "Analysis of Anisotropic Plates," *Journal of Composite Materials*, Vol. 3, 1969, pp. 148-165.

[3]Viswanathan, M. T., and Baker, L. L., "Elastic Stability of Laminated, Flat and Curved, Long Rectangular Plates Subjected to Combined Inplane Loads," NASA CR-2330, June 1974.

[4]Almroth, B. O., Brogan, F. A., Meller, E., Zele, F., and Petersen, H. T., "Collapse Analysis for Shells of General Shape," AFFDL-TR-71-8, March 1973.

[5]Noor, A. K. and Mathers, M. D., "Shear-Flexible Finite-Element Models of Laminated Composite Plates and Shells," NASA TN D-8044, Dec. 1975.

[6]Smirnov, A. I., "Laminated Panel Flutter in Supersonic Flow," *Izvestiya Vuz. Aviatsionnaya Tekhnika*, Vol. II, 1968, pp. 33-38.

[7]Librescu, L. and Badoiu, T., "Supersonic Flutter of Plane, Rectangular, Anisotropic Heterogeneous Structures," NASA TT F-15, 890, Aug. 1974.

[8]Rankumar, R. L., "Flutter Analysis of Flat Rectangular Anisotropic Panels in a High Mach Number Supersonic Flow," M.S. Thesis, Virginia Polytechnic Institute and State University, Blacksburg, Va., 1974.

[9]Erickson, Larry L., "Supersonic Flutter of Flat Rectangular Orthotropic Panels Elastically Restrained Against Edge Rotation," NASA TN D-3500, 1966.

[10]Ashton, J. E. and Whitney, J. M., *Theory of Laminated Plates*, Technomic Publishing Co., Inc., 1970.

[11]Sawyer, James W., "Flutter of Laminated Plates in Supersonic Flow," NASA TM X-72800, Nov. 1975.

[12]Hedgepeth, J. M., "Flutter of Rectangular Simply Supported Panels at High Supersonic Speeds," *Journal of Aeronautical Sciences*, Vol. 24, Aug. 1957, pp. 563-573, 586.

[13]Fung, Y, C., *Foundations of Solid Mechanics*, Prentice-Hall, Englewood Cliffs, N.J., 1965, pp. 338-339.

[14]Williams, J.C. and Mikulas, M.M. Jr., "Analytical and Experimental Study of Structurally Efficient Composite Hat-Stiffened Panels Loaded in Axial Compression," AIAA Paper 75-754, *AIAA/ASME/SAE 16th Structures, Structural Dynamics, and Materials Conference*, Denver, Colo., May 1975.

From the AIAA Progress in Astronautics and Aeronautics Series . . .

AEROACOUSTICS: FAN, STOL, AND BOUNDARY LAYER NOISE; SONIC BOOM; AEROACOUSTIC INSTRUMENTATION—v. 38

Edited by Henry T. Nagamatsu, General Electric Research and Development Center; Jack V. O'Keefe, The Boeing Company; and Ira R. Schwartz, NASA Ames Development Center
A companion to Aeroacoustics: Jet and Combustion Noise; Duct Acoustics, volume 37 in the series.

Twenty-nine papers, with summaries of panel discussions, comprise this volume, covering fan noise, STOL and rotor noise, acoustics of boundary layers and structural response, broadband noise generation, airfoil-wake interactions, blade spacing, supersonic fans, and inlet geometry. Studies of STOL and rotor noise cover mechanisms and prediction, suppression, spectral trends, and an engine-over-the-wing concept. Structural phenomena include panel response, high-temperature fatigue, and reentry vehicle loads, and boundary layer studies examine attached and separated turbulent pressure fluctuations, supersonic and hypersonic.

Sonic boom studies examine high-altitude overpressure, space shuttle boom, a low-boom supersonic transport, shock wave distortion, nonlinear acoustics, and far-field effects. Instrumentation includes directional microphone, jet flow source location, various sensors, shear flow measurement, laser velocimeters, and comparisons of wind tunnel and flight test data.

509 pp. 6 x 9, illus. $19.00 Mem. $30.00 List

TO ORDER WRITE: Publications Dept., AIAA, 1290 Avenue of the Americas, New York, N. Y. 10019